

Correlation of Eocene–Oligocene marine and continental records: orbital cyclicity, magnetostratigraphy and sequence stratigraphy of the Solent Group, Isle of Wight, UK

A. S. GALE^{1,2}, J. M. HUGGETT³, H. PÄLIKE⁴, E. LAURIE¹, E. A. HAILWOOD⁵ & J. HARDENBOL⁶

¹*Department of Earth and Environmental Sciences, University of Greenwich, Medway Campus, Chatham Maritime ME4 4TB, UK*

²*Department of Palaeontology, Natural History Museum, Cromwell Road, London SW7 5BD, UK (e-mail: asg@nhm.ac.uk)*

³*Department of Mineralogy, Natural History Museum, Cromwell Road, London SW7 5BD, UK*

⁴*Department of Geology and Geochemistry, Stockholm University, S-10691, Stockholm, Sweden*

⁵*Core Magnetics, The Green, Sedbergh LA10 5JS, UK*

⁶*GSC Inc., 826 Plainwood Drive, Houston, TX 77079, USA*

Abstract: The magnetostratigraphy, clay mineralogy, cyclostratigraphy and sequence stratigraphy of the estuarine and continental Solent Group (Isle of Wight, Hampshire Basin, UK), which is of Late Eocene–Early Oligocene age, were investigated. A new magnetostratigraphy for the Solent Group is correlated to the chronostratigraphic standard using limited biostratigraphical data, and it is concluded that the base of the Oligocene falls close to the base of the Bembridge Limestone Formation. A long time-series of clay mineral XRD data was generated, which shows striking variation in illitic clay abundance. Illite is interpreted to have formed in gley palaeosols through repeated wetting and drying in response to high seasonality. High illitic clay values are tuned to *c.* 400 ka eccentricity maxima to develop an age model. In addition to a very strong *c.* 400 ka signal in the data, spectral analysis of the clay data also confirms the influence of short eccentricity (*c.* 100 ka) and obliquity (*c.* 40 ka) cycles. The succession displays seven conspicuous 10–20 m thick sequences, which represent transitions from transgressive estuarine environments through highstand floodplains to freshwater lakes. The sequences correspond exactly to the long eccentricity (*c.* 400 ka) cycles. A sea-level curve is derived using the amount of incision as a minimum measure of eustatic fall, but there is no evidence of a major eustatic drop of 30–90 m corresponding to the early Oligocene glaciation of Antarctica. It is likely that incision was suppressed by rapid rates of subsidence.

Correlation between coeval marine and continental successions has been one of the most difficult challenges facing stratigraphers. In addition to the traditional methods based on the interdigitation of contrasting facies and faunas, developments in magnetostratigraphy, carbon-isotope stratigraphy, chemostratigraphy, sequence stratigraphy and astronomical cyclostratigraphy provide extensive new tools with which to resolve difficult correlation problems. Extraordinarily precise correlations, of the order of tens of thousands of years, can be achieved using these methods. For example, correlation of the Late Miocene–Pliocene continental succession of the Ptolemais area of NW Greece with the marine record is now possible on the scale of individual obliquity (41 ka) cycles (e.g. Van Vugt *et al.* 1998; Steenbrink *et al.* 1999). The deep marine Cenozoic succession is known in increasing detail from Deep Sea Drilling Project and Ocean Drilling Program records, and an orbitally tuned succession, precisely calibrated with bio- and magnetostratigraphy, provides a template for the last 33 Ma (Shackleton *et al.* 1995, 1999). The present study applies orbital tuning, magnetostratigraphy and sequence stratigraphy to a dominantly continental succession of Late Eocene–Early Oligocene age.

The Solent Group is a succession of brackish and freshwater clays, sands and thin freshwater limestones of Late Eocene to Early Oligocene age, with a maximum thickness of 200 m, which is preserved only in the central part of the Hampshire Basin, in southern Hampshire and the Isle of Wight (Figs. 1 and 2). The

succession represents the youngest Palaeogene strata present onshore in the UK. Important general descriptions of the succession have been given by Forbes (1853) and White (1921), and the lithostratigraphy was thoroughly revised by Insole & Daley (1985), who named the Solent Group and divided it into three component formations (Headon Hill, Bembridge, Bouldnor) with numerous members (Fig. 2). The stratigraphy of the Bembridge Limestone was revised by Daley & Edwards (1990) and an extensive review of all previous work on the Tertiary deposits of the Isle of Wight has been published by Daley (1999).

Research on the Solent Group has focused on its palaeontology. Algae, palynomorphs, nannofossils, dinoflagellates, macroscopic plants and wood, foraminiferans, molluscs, ostracodes, crustaceans, insects, arachnids, fish, amphibians, reptiles and mammals have all been described in about 100 papers, whereas there have been fewer than 10 articles on the sedimentology and mineralogy (see references given by Daley 1999). The clay mineralogy of the succession was outlined by Gilkes (1968) and the carbonate sedimentology and palaeoenvironments of the Bembridge Limestone have been studied in detail by Armenteros *et al.* (1997).

This study concentrated on the Solent Group exposed in Whitecliff and Howgate Bays, between Sandown and Bembridge in the east of the Isle of Wight [SZ 641862–649870]. Here, 132 m of clays, silts, sands and limestones comprising the entire Headon Hill Formation, the Bembridge Limestone Formation

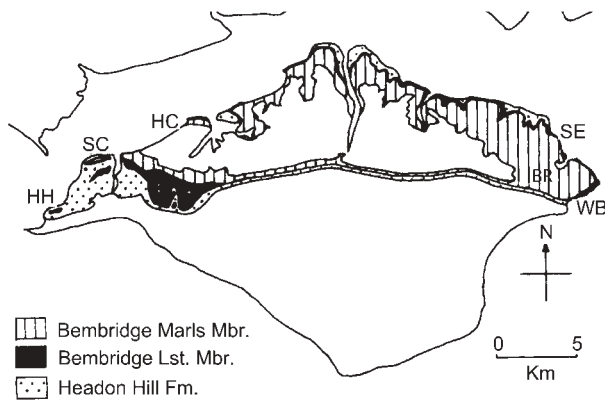


Fig. 1. Map of Isle of Wight to show outcrop of Solent Group, Bembridge Limestone, Headon Hill Formation and Bouldnor Formation and localities mentioned in the text. HH, Headon Hill; SC, Sconce; HC, Hamstead Cliff; SE, Seagrove; BR, Brading; WB, Whitecliff Bay.

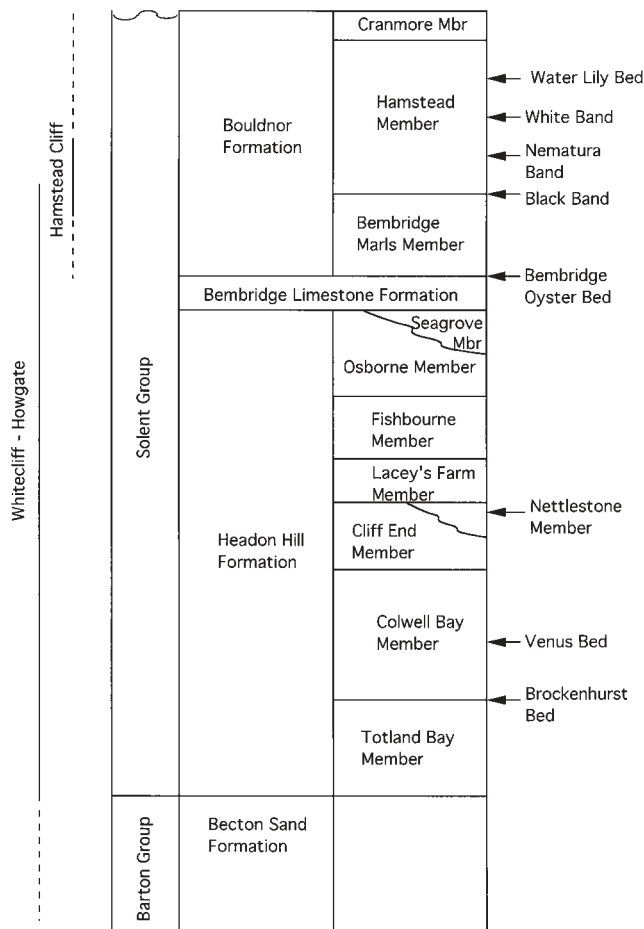


Fig. 2. Stratigraphy of the Solent Group in the Isle of Wight, after Insole & Daley (1985). The lines to the left of the column show the ranges of Whitecliff Bay and Hamstead Cliff sections; continuous lines indicate the intervals we have sampled for this study.

and the lower part of the Bouldnor Formation (White 1921; Daley 1972; Insole & Daley 1985) are exposed in cliffs, and occasionally on the foreshore in Whitecliff Bay (Fig. 3). The Solent Group succession here is the thickest exposed (Insole & Daley 1985, fig. 6), although the highest part of the Totland Bay

Member of the Headon Hill Formation, including the *vectensis-nanus* mammal zone (Hooker 1992, fig. 25.2) is missing beneath the Brockenhurst Bed at the base of the Colwell Bay Member, probably because of a hiatus.

Exceptionally clean exposures were available during the stormy winter and spring of 2000–2001 when the Whitecliff Bay succession was logged and sampled. To develop a regional picture, the important successions at Headon Hill [SZ 305856–317863], between Sconce and Colwell Bay in the western Isle of Wight [SZ 329881–337897], and between Seaview and St. Helens [SZ 638897–634907], 6 km north of Whitecliff, were also studied. Additionally, part of the Bembridge Marls and Hamstead Members of the Bouldnor Formation at Hamstead Cliff [SZ 400918–403920] were sampled for magnetostratigraphy.

Biostratigraphy

The chronostratigraphical time scale for the Eocene–Oligocene is based upon marine nannofossils, planktic foraminiferans and the magnetostratigraphic record (e.g. Berggren *et al.* 1995; Cande & Kent 1995). The base of the Oligocene is defined by the extinction of the planktic foraminiferan *Hantkenina* (Berggren *et al.* 1995), which predated shifts to heavier values of $\delta^{18}\text{O}$ and $\delta^{13}\text{C}$ (Zachos *et al.* 1996) by *c.* 100 ka. The isotope events are coincident with the base of magnetochron 13n. To date precisely any given succession it is necessary to correlate accurately to at least some of these events. As the Solent Group is largely non-marine and of very restricted brackish facies, planktic foraminiferans are totally absent. Nannofossils are found, however, at two marine horizons, the Brockenhurst Bed (Colwell Bay Member, Headon Hill Formation) and the Corbula Beds (Cranmore Member, Bouldnor Formation; Martini 1970; Aubry 1985; Fig. 2). The Brockenhurst Bed has been previously dated at NP19–20 (Martini 1970) and the Corbula Beds at NP23 (Aubry 1985). J. Backman (University of Stockholm, Sweden) confirmed the presence of *Discoaster saipanensis* and *Ismolithus recurvus* in the Brockenhurst Bed, and thus the NP19–20 age.

Hooker (1992) identified five mammal zones (MP17–21) in the Solent Group of the Isle of Wight (Fig. 3), and these are also recognized in Belgium, Germany (Rhine Graben) and the Paris Basin. In continental Europe, several of these mammaliferous deposits either yield nannofossils or are intercalated with nannofossil-bearing sediments (Hooker 1992). The Argiles Vertes de Romainville in the Paris Basin yield nannofossils indicating NP22, and their lateral equivalent, the Calcaire de Brie, contains mammals diagnostic of MP21, supported by additional information from Belgium and the Rhine Graben, Germany (Hooker 1992). This date is supported by dinoflagellate correlation between the Nematura Bed (Hamstead Member, Bouldnor Formation) in the NW Isle of Wight and the Argiles Vertes de Romainville (Liengjaren *et al.* 1980). The following facts can be established by means of direct and indirect biostratigraphic correlation. (1) The Brockenhurst Bed in Whitecliff Bay contains nannofossils diagnostic of zones NP19–20, and occurs low within MP18. (2) The mammal zone MP21 is at least partly coincident with the nannofossil zone NP22. Thus, the level of the Nematura Bed in the NW Isle of Wight is within NP22, but not necessarily at the base of that zone. This is corroborated by dinoflagellate data. (3) The Corbula Beds in the Cranmore Member of Hamstead Cliff (uppermost Solent Group) occur within NP23, supported by evidence from dinoflagellates.

There have been a number of recent attempts to identify the position of the Eocene–Oligocene boundary within the Solent

duration of this gap at 350 ka, and argued that it must represent the sea-level fall associated with isotope event Oi-1, close to the base of the Oligocene and coincident with the Grand Coupure, a major turnover in mammal faunas. However, the position of the critical magnetochron C13n shown by Hooker *et al.* (2004, fig. 3) is entirely hypothetical in the UK successions, as are the magnitudes of the supposed hiatuses. The position of the base of the Oligocene in the Solent Group of the Isle of Wight therefore remains very uncertain.

Magnetostratigraphy

The magnetostratigraphy of the Whitecliff Bay and lower Hamstead Cliff sections was investigated to establish the record of geomagnetic polarity reversals during deposition. Correlation of the observed polarity sequence with the radiometrically calibrated Eocene–Oligocene magnetic polarity time scale, using available biostratigraphic constraints, allows successive normal and reverse polarity intervals in the sections to be calibrated with specific geomagnetic chrons (Hailwood 1989). The positions of individual chron boundaries in the section then provide numerical ages for these events.

Sampling and methods

A set of oriented samples was taken for palaeomagnetic analyses, using the copper tube method of Townsend & Hailwood (1985). Average sample spacing was 1.5 m in the upper two-thirds of the section and 3 m in the lower third. One or more 25 mm right-cylindrical specimens were cut from each sample. Each specimen was subjected to incremental thermal demagnetization analysis, to remove spurious components of magnetization associated with sampling, handling and laboratory storage, and to isolate the different geologically significant components. Palaeomagnetic measurements were made on an Agico high-sensitivity automated spinner magnetometer and demagnetization was carried out with a Magnetic Measurements MMTD18 thermal demagnetizer. Temperature increments in the range 25 °C to 75 °C were used, up to a maximum temperature of 550 °C, by which stage the magnetic intensity was typically reduced to <5% of the initial value and directions of magnetization began to change erratically.

The magnetometer had an effective noise level of 0.002 mA m⁻¹ and directions of magnetization were measured with a typical precision of *c.* 1–3° at all but the highest demagnetization temperatures, where the precision reduced to *c.* 5°. The intensity of natural remanent magnetization (NRM) ranged from 0.02 to 0.04 mA m⁻¹ for most of the section, with lower values in sand and carbonate lithologies and higher values in clay-rich lithologies. However, an interval of significantly enhanced NRM intensity was identified in the middle to lower part of the Colwell Bay Member (*c.* 107–120 m below datum).

Principal component analysis (PCA) of the demagnetization data (Kirschvink 1980) identified two significant components of magnetization in the majority of samples. The low-temperature component was typically defined at temperatures below 300 °C and its direction (before structural correction) was close to that of the modern geomagnetic field in this region. This component is a viscous magnetization acquired through prolonged exposure of the sediments to the geomagnetic field during the present (Bruhnes) normal polarity magnetic chron.

In most samples, the high-temperature component of magnetization was best defined in the temperature range 320–550 °C. Application of a palaeomagnetic fold-test (McElhinny 1964) demonstrates that this component clearly predates structural tilting of the section and it is considered, therefore, to represent the primary magnetization of the formation. Microscope examinations, isothermal remanent magnetization (IRM) acquisition analyses and three-component IRM demagnetization analyses (Lowrie 1990) on representative sets of samples indicate that the principal carrier of remanent magnetism in these sediments is magnetite, probably of detrital origin.

Discrete high-temperature components of magnetization could not be

identified in about 10% of the samples. However, in all such cases, the polarity of the high-temperature component could still be clearly defined by fitting a great circle to the directional trend of the magnetic vector during successive demagnetization steps for the temperature range 320–550 °C. For all such samples, the trend was towards a negative inclination and southerly declination, indicating a reversed polarity.

The polarity determination for each sample was assigned to one of four categories, to provide a measure of its quality. Categories 1–3 refer to samples for which the high-temperature direction of magnetization was determined by PCA and for which the maximum angular deviation (MAD) values lie in the ranges <5, 5–15 and >15°, respectively. Category 0 applies to samples in which the polarity of this component was determined from analyses of directional trends.

Stratigraphic plots of the declination and inclination of the high-temperature magnetic vectors are shown in columns 2 and 3 of Figure 3. The reliability category is plotted in column 4 and the magnetic polarity in column 5.

Most of the upper two-thirds of the section (Cliff End to Seagrove Bay Members of the Headon Hill Formation, together with the Bembridge Limestone and Bouldnor Formations) is characterized by a reversed magnetic polarity (negative inclination and southerly declination). However, this interval encompasses a single well-defined normal polarity zone, which extends from the upper part of the Bembridge Limestone into the lower quarter of the Bembridge Marls, a total thickness of some 6 m (Fig. 3). This is called here the 'Bembridge normal polarity zone'. The upper and lower limits of this zone are well constrained by a close set of samples and the palaeomagnetic determinations for all samples are of high quality (Category 1).

Four further short normal or 'intermediate' polarity intervals were observed in the upper two-thirds of the section (Fig. 3). However, each of these is based on a single specimen only and because of relatively wide sample spacing in these parts of the section, the stratigraphic extension of the intervals is poorly constrained. Furthermore, the quality of the palaeomagnetic determinations for all four intervals is relatively poor (mostly Category 3). It is possible that these intervals represent very short period normal polarity magnetic events, but in view of the above limitations, particularly the absence of confirmation from duplicate specimens, their reliability must be considered questionable.

The lower third of the section is characterized by a dominantly normal polarity throughout. This interval lies in the lower half of the Headon Hill Formation and is referred to here as the 'Headon Hill normal polarity zone'. Although sample spacing is relatively wide within this zone, closer sampling across its upper and lower boundaries allows their positions to be defined to within ±1 m.

Recent magnetic polarity time scales (e.g. Berggren *et al.* 1995) indicate that geomagnetic Chron C15n lies within nannofossil zone NP19–20 and Chron C13n lies in the middle part of NP21. The assignment of the Brockenhurst Bed (at the base of the Headon Hill normal polarity zone) to NP19–20 (see above) indicates that this normal zone must represent Chron C15n. The identification of mammal zone MP21, which is at least partly coincident with nannofossil zone NP22 (see above), at the base of the Upper Hamstead Member indicates that this level must postdate geomagnetic Chron C13n. Therefore, the Bembridge normal polarity zone represents Chron C13n.

Sequence stratigraphy

Sequences (transgressive–regressive facies cycles and bounding unconformities) are identified in the Solent Group of the Isle of Wight from sedimentological criteria, supported by palaeontological and mineralogical data. The locality lay on the edge of a coastal plain developed around the southern side of the proto-Solent estuary during Late Eocene–Early Oligocene times (Daley 1972; Keene 1977), and marine and brackish inundations in the succession are conspicuous. Mollusc, ostracode and vertebrate faunas and floras provide important palaeoenvironmental evidence, and allow detailed reconstruction of salinities in particular (Fig. 4), the nature of freshwater bodies, palaeoclimates, and the nature and extent of vegetation cover (e.g. Keene

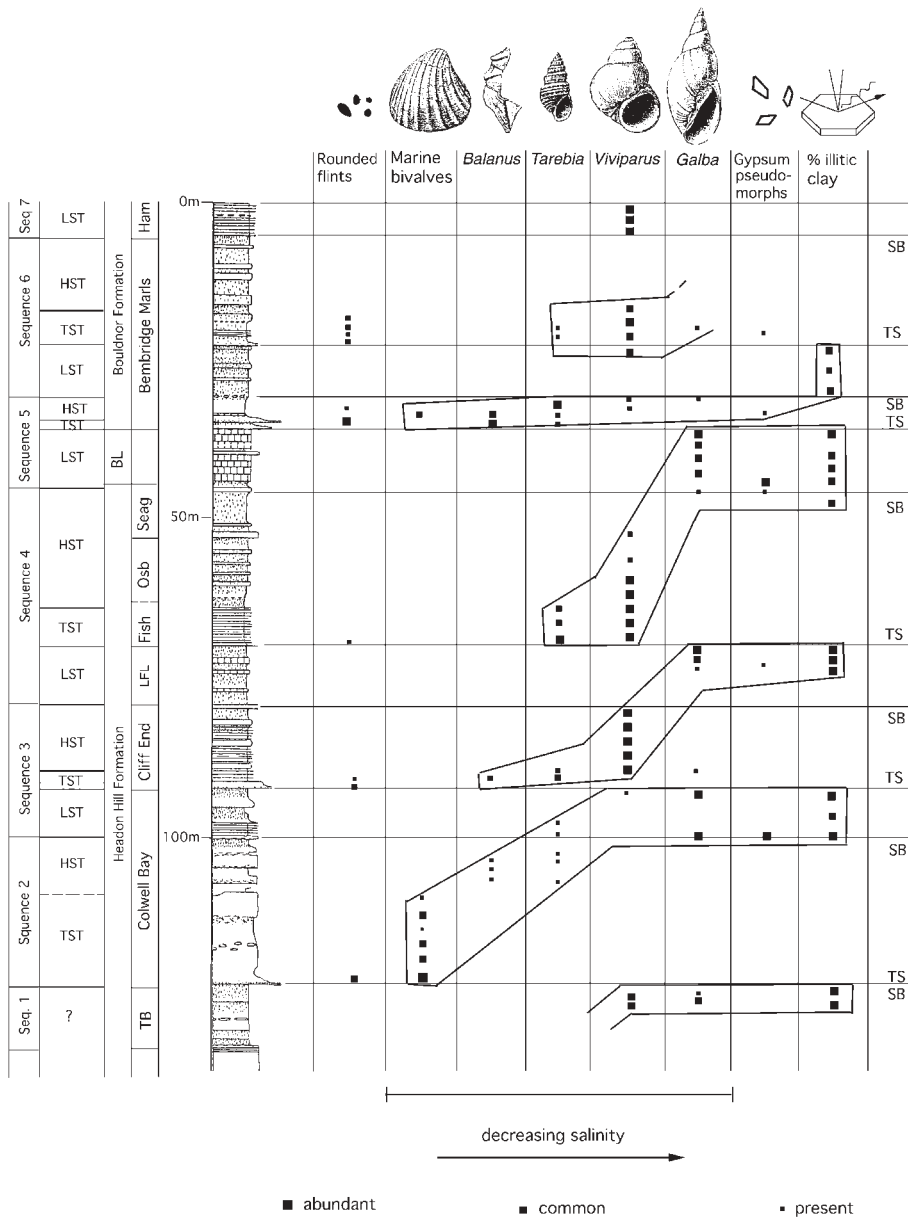


Fig. 4. Sequence stratigraphy of the Solent Group in Whitecliff Bay showing selected sedimentological, palaeontological and mineralogical evidence. The pattern of brackish to marine transgressive systems tracts, fluvialite pedogenic highstands, and lacustrine, carbonate-rich lowstands is repeated through Sequences 1–5 both here and elsewhere in the Isle of Wight. Above the Bembridge Limestone, limestones disappear and *Galba* is virtually absent. LST, lowstand system tract; HST, highstand system tract; TST, transgressive system tract; TB, Totland Bay Member; LFL, Lacey’s Farm Limestone; BL, Bembridge Limestone; SB, sequence boundary; TS, transgressive surface.

1977; Paul 1989; Hooker *et al.* 1995). Additional evidence comes from the occurrence of evaporite pseudomorphs (Armenteros *et al.* 1997), palaeosols and quantitative clay mineralogy (see above; also Huggett *et al.* 2001; Huggett & Cuadros 2005).

Although sequences are well defined, it has proved very difficult to place the Solent Group succession within described estuarine facies models, probably because the sediment is so ubiquitously fine. Silty clays, marls and limestones were deposited in a low-energy, low-gradient estuarine system (Armenteros *et al.* 1997). Seven sequences are identified in the Solent Group of Whitecliff Bay (Fig. 4), and traced to other outcrops on the island (Fig. 5). The sequences are numbered informally from oldest to youngest (Sequences 1–7).

Transgressive and highstand systems tracts

Transgressive deposits rest upon an erosionally truncated surface of the underlying lowstand (more rarely highstand) and comprise a sparse basal conglomerate containing flint pebbles (Fig. 4),

overlain by silts and fine sands. The flints are highly rounded and percussion scarred, and were probably derived from earlier Eocene conglomeratic lags, such as those in the London Clay Formation and Bracklesham Group (Gale *et al.* 1999). The transgressive systems tracts are the most marine-influenced parts of the Solent Group succession, as shown by their molluscan faunas (Fig. 4), which indicate that fully marine conditions were achieved only during deposition of the Brockenhurst Bed and overlying 13 m of sands (Sequence 2). The lower part of the Bembridge Marls (Sequence 5) includes a few marine species (e.g. the bivalve *Nucula*) in a fauna dominated by brackish forms including cirripedes and *Tarebia* (Daley 1972, 1999). Brackish molluscs occur dominantly in the lower part of transgressive sequences; for example, in the Fishbourne Member (Sequence 4) the basal silts and fine sands of each 2 m cycle contain the brackish gastropod *Tarebia* (Fig. 4) whereas the upper clays yield only the freshwater *Viviparus*. This prosobranch gastropod has gills and is therefore entirely restricted to permanent freshwater bodies (Paul 1989).

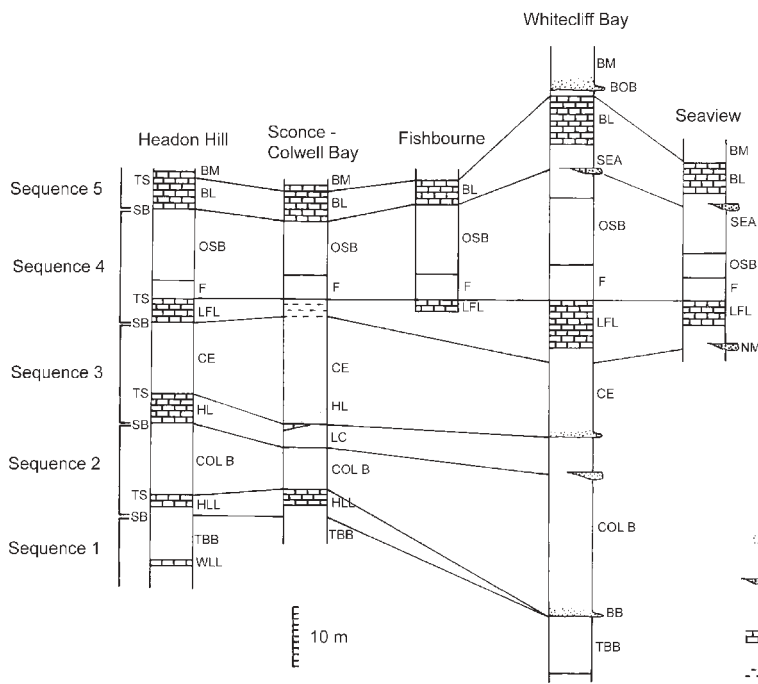


Fig. 5. Correlation of Sequences 2–5 in the Solent Group around the Isle of Wight. WLL, Warden Ledge Limestone; TBB, Totland Bay Member; HLL, How Ledge Limestone; COL B, Colwell Bay Member; HL, Hatherwood Limestone; CE, Cliff End Member; LFL, Lacey's Farm Limestone; F, Fishbourne Member; OSB, Osborne Member; BL, Bembridge Limestone; BM, Bembridge Marls; LC, Linstone Chine Member; SEA, Seagrove Member; BOB, Bembridge Oyster Bed; NM, Nettlestone Member. SB, sequence boundary; TS, transgressive surface.

Both transgressive and highstand deposits are made up of 1–3 m thick, erosionally based fining upwards cycles (Fig. 6). The lower part of each cycle comprises massive silt or very fine sand, rarely rippled or planar laminated, which passes up into silty clay. Thin lenses (0.01–0.05 m) of mollusc shells occur. In the lower part of each sequence, the fining upward cycles are terminated by bioturbated clays, but as sea level fell, the upper parts of cycles are increasingly pedogenized, and mottled gley and pseudogley palaeosols terminate each cycle (Huggett *et al.* 2001). The cycles are interpreted as representing shallow (2–4 m deep) tidal channels, cut into the flood plain of the proto-Solent, which were progressively infilled and eventually abandoned. In the transgressive and lower highstand systems tracts, the deeper parts of the channels were infilled with higher salinity flood tide waters, and therefore contain brackish species. Channels were abandoned to form unvegetated, low-salinity supratidal flats. Later in the highstand, the channels received only freshwater from riverine input (as evidenced by the transported *Viviparus*) and densely vegetated soils developed when they were abandoned.

Sequence boundaries and early lowstand deposits

Sequence boundaries are represented by marked facies changes in Whitecliff Bay, but incision is here relatively inconspicuous. In the north of the island, closer to the position of the proto-Solent channel, early lowstand deposits comprise fluvial sands, gravels and lenses of conglomerate, which rest erosionally upon sequence boundaries cut into pedogenic silty clays of the preceding highstand deposits. The conglomerates contain flints and limestone intraclasts; the sand matrix is full of finely comminuted shell debris (now mouldic), and the freshwater gastropod *Viviparus* is abundant.

Conglomeratic channel lags are well developed at the bases of Sequences 3–5 and a complex intraclastic lag in the Colwell Bay Member is exposed on the foreshore in Whitecliff Bay (97–100 m, Fig. 4). At Seaview (Fig. 5; [SZ 630917]), the early lowstand deposits of Sequence 4 are represented by a 6 m thick

shelly fluvial sand (the 'Nettlestone Beds' of Forbes 1853), herein referred to as the Nettlestone Member (Fig. 5). In the upper part this contains intraclasts, worn bone fragments and rare subangular chalk flints. In the northeastern Isle of Wight the Bembridge Limestone is underlain locally by gravels and conglomerates (Insole & Daley 1985), which represent early lowstand deposits of Sequence 5 (Fig. 7). Several metres of conglomerates containing abundant subrounded and soil-weathered flints (up to 0.1 m long) are present beneath the Bembridge Limestone at Cliff Close, Brading [SZ 609873] (White 1921), and at Horestone Point, south of Seaview [SZ 634507], a 1 m thick flint conglomerate is present beneath the Bembridge Limestone. These deposits demonstrate that significant downcutting took place at this sequence boundary, which was sufficient to cause extensive erosion of the older Palaeogene sediments and the Chalk, and flint conglomerates were transported northwards towards the proto-Solent in newly incised fluvial channels.

Late lowstand deposits

Later lowstand deposits in the lower Solent Group (Headon Hill and Bembridge Limestone Formations) in Whitecliff Bay consist predominantly of green–grey silty pedogenic clays and freshwater marls and biogenic limestones representing lacustrine and palustrine environments, broadly similar to but often less calcareous than the Bembridge Limestone (Armenteros *et al.* 1997). In Whitecliff Bay, the limestone facies is developed only in Sequences 4 (Lacey's Farm Lst) and 5 (Bembridge Lst), but at Headon Hill in the western Isle of Wight (Fig. 5) limestones are better developed and occur also in Sequences 2 (How Ledge Lst) and 3 (Hatherwood Lst). The limestones and clays formed in lakes on a coastal plain of very low relief, with rare, brief brackish and marine incursions particularly in north and west Wight (e.g. Paul 1989; Armenteros *et al.* 1997). The limestones are conspicuously cyclic on a metre scale and each terminates

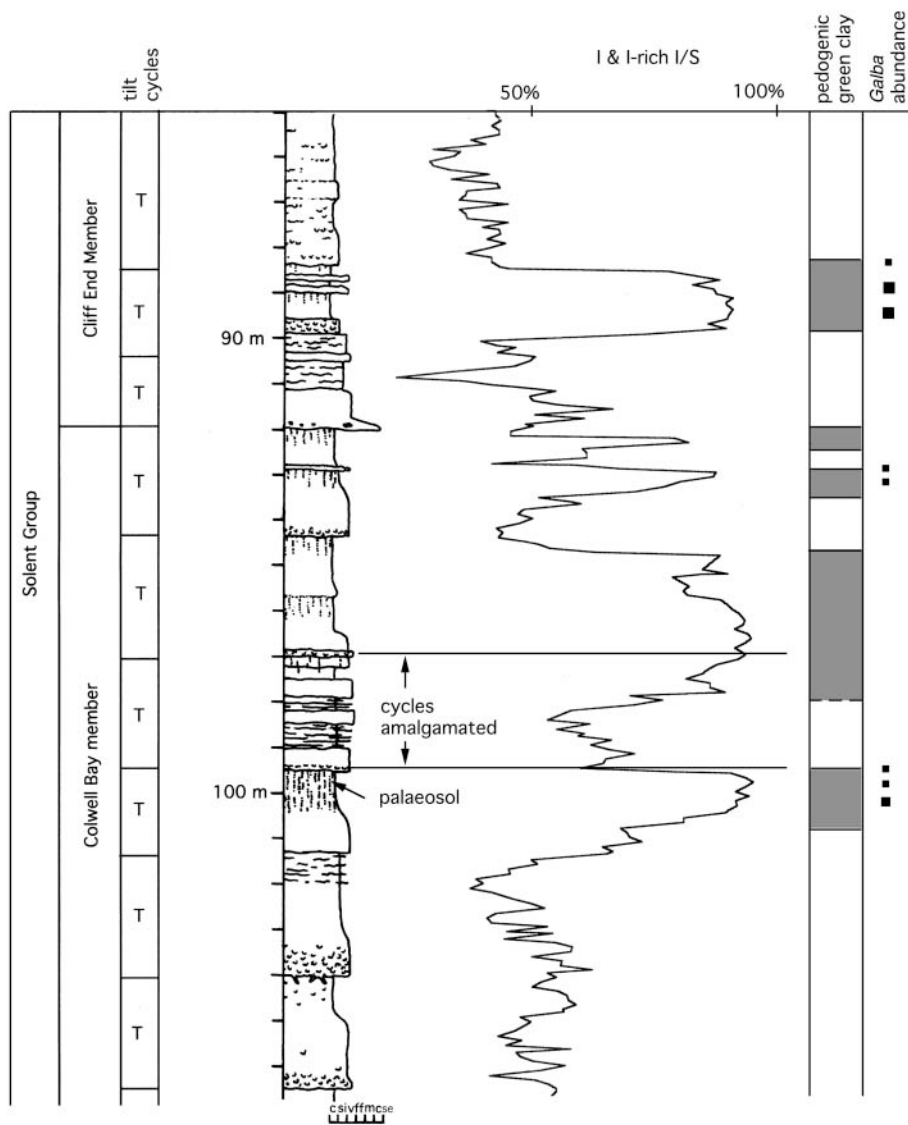


Fig. 6. Stratigraphy and sedimentology of the upper part of the Colwell Bay Member and the lower part of the Cliff End Member, Whitecliff Bay. The succession comprises 2–3 m thick fining upwards cycles (fine sand–silty clay, labelled T), commonly with a mollusc shell lag at the base.

with a palaeosol indicating shallowing upwards (Armenteros *et al.* 1997).

These later lowstand deposits are interpreted as representing periods during which the area was isolated from the main proto-Solent drainage system, and ephemeral carbonate lakes developed across a marshy, low-relief coastal plain. In the SW of the island, the plain was wooded, as evidenced by arboreal mammal and gastropod faunas (Hooker 1992; Hooker *et al.* 1995). Water body development was probably controlled seasonally, and repeated, alternate wetting and drying led to the transformation of smectite-rich illite–smectite to illite-rich illite–smectite in gley palaeosols (Huggett *et al.* 2001; Huggett & Cuadros 2005) and provided an ideal habitat for the air-breathing pulmonate snail *Galba* (Fig. 4), which is abundant in the limestones. A detailed knowledge exists of the habitat preferences of this genus because the closely related living *G. truncatula* (Linnaeus) has received detailed study, as it is secondary host to the liver fluke. The genus is well adapted to ephemeral pools and wet meadows because it can survive desiccation (Ellis 1969). Arid periods during early lowstands led to the widespread formation of gypsum in palaeosols, now preserved as calcite pseudomorphs

(Huggett *et al.* 2001). These are notably well developed in the Colwell Bay Member (–100 m, Fig. 4) and immediately beneath the Bembridge Limestone (Fig. 7). These beds represent periods of maximum evaporation, and probably correlate with more extensive evaporite-forming events known from the Paris Basin (second and first gypse respectively of Pomerol 1982).

Magnitude of sea-level changes

The amount of erosional incision associated with successive sequence boundaries is estimated from the thickness of the lowstand deposits above the sequence boundary in the sequences present in Whitecliff Bay, and is used as a minimum measure of sea-level fall (Fig. 8; Table 1; see Gale *et al.* 2002). Values are also given from the correlative Headon Hill succession in the west of the island (Fig. 5) for comparison. The proximity to sea level, rapidity of sea-level fall and softness of incised sediment are all features that increase the likelihood that these values are close to the actual eustatic fall in sea level (Schumm 1993). However, the amount of incision can be suppressed dramatically by high subsidence rates (Davies & Gibling 2003), which may

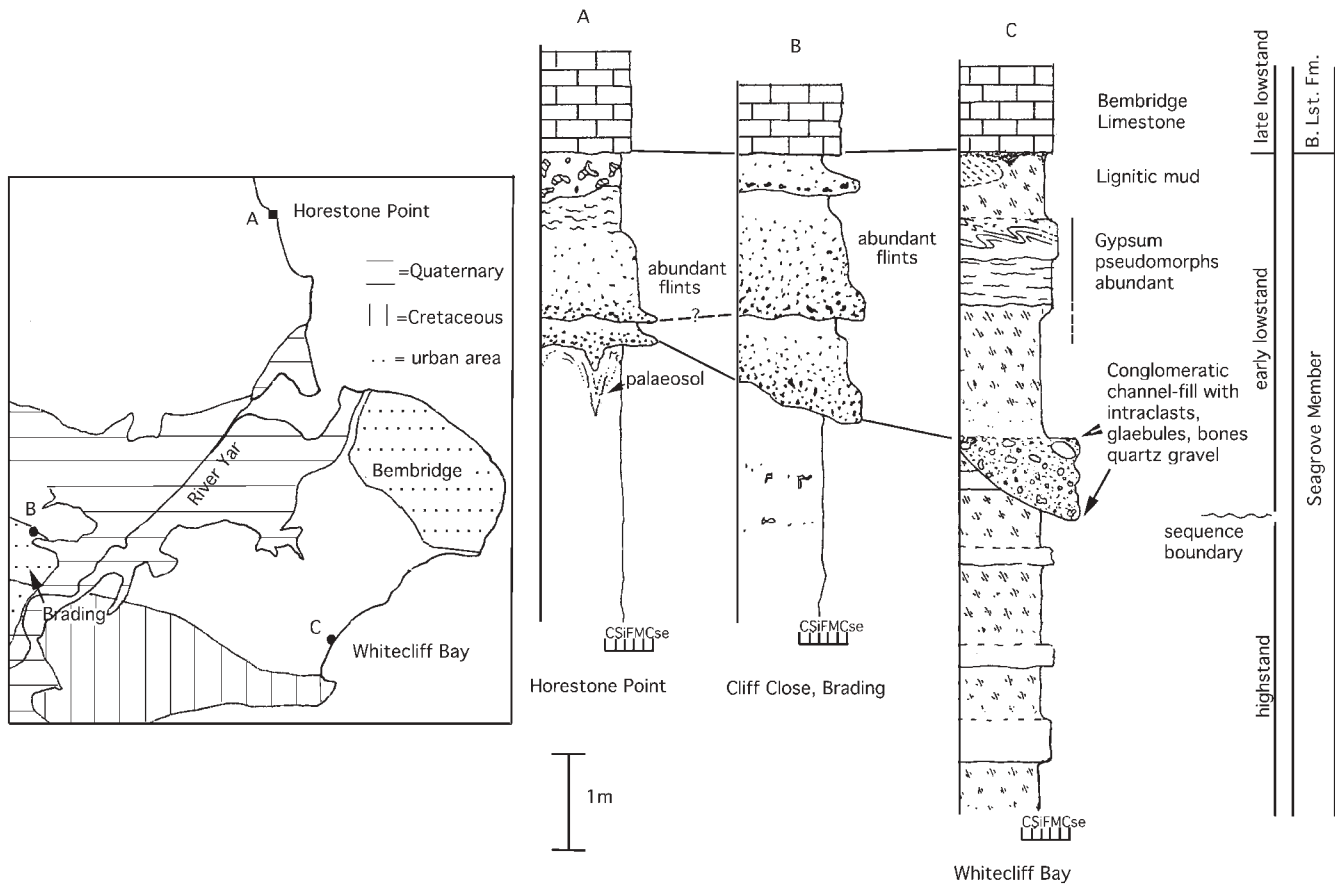


Fig. 7. Stratigraphy and correlation of the uppermost Seagrove Bay Member and basal Bembridge Limestone Formation, eastern Isle of Wight. The base of the channel is interpreted as a sequence boundary, and contains successive fining upwards fluvialite flint conglomerates at Horestone and Brading, and an intraclastic fill with glaebules and worn mammal teeth in Whitecliff Bay. The sea-level fall at the sequence boundary shown is the largest in the succession (minimum fall of 15 m), and is probably a reflection of the Oi-1a event, which involved enlargement of the Antarctic ice sheet.

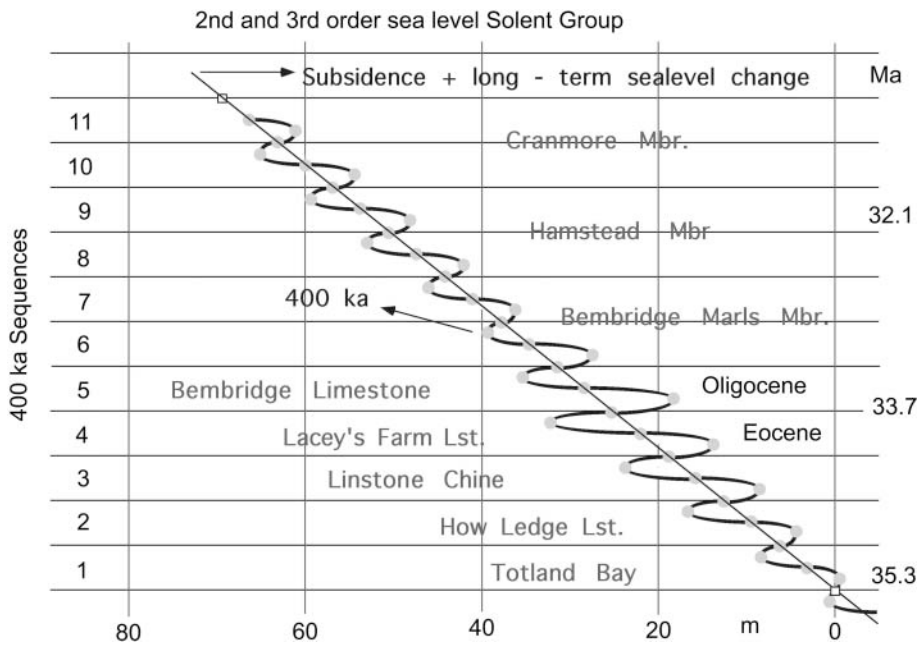


Fig. 8. Relative sea-level curve and eustatic rise through the succession in Whitecliff Bay. The amount of fall and rise on individual 400 ka cycles is calculated from the amount of incision on sequence boundaries. The method has been described by Gale *et al.* (2002).

Table 1. Incision associated with sequence boundaries in the Solent Group, taken from thickness of lowstands

Sequence number	Incision, Whitecliff Bay (m)	Incision, Headon Hill (m)
7	2+	
6	8	
5	14	10+
4	10	7
3	8	6
2		3
1		1

have been a factor in the Solent Group where accumulation rates of 50–75 m Ma⁻¹ can be estimated.

The sea-level curve derived from incision data shows a progressive increase in the magnitude of change through the lower Solent Group, from a 3 m fall in Sequence 2 to nearly 15 m in Sequence 5 at the level of the Bembridge Limestone. Values fall rapidly in the overlying Bembridge Marls to 7 m and 2 m in Sequences 6 and 7, respectively.

Clay mineralogy

Sampling and methods

XRD analysis of the clay fraction (<2 µm) was carried out using a Philips 1820 automated X-ray diffractometer with Cu Kα radiation. A total of 740 samples from Whitecliff Bay were analysed from a thickness of 124 m, a mean spacing of 0.17 m. Samples were scanned air-dried, after solvation with glycol and heating for 2 h at 400 °C and 550 °C. Reflection intensity factors for semi-quantification were determined from XRD data for known mixtures of standard clays. Accuracy for these is *c.* ±20% of the given value, and precision is *c.* ±5%. Limestones were first leached with 30% acetic acid and the <2 µm fraction of the resulting insoluble residue was analysed.

Clay mineral succession

Although clay mineral percentages have been plotted (Fig. 9) these were used only to determine trends because they are semi-quantitative. The clay mineral suite is dominated by mixed layer illite–smectite clays: illite-rich illite–smectite with 80% illite and 20% smectite layers (for brevity termed illite) and more highly expandable illite–smectite clays (for brevity termed smectite), plus kaolinite and minor chlorite. Selected illite-rich and smectite-rich XRD patterns have been modelled using NEW-MOD™ to determine the precise illite–smectite compositions and their abundances (Huggett & Cuadros 2005). These data indicate that many illite–smectite compositions are present but that it is reasonable for the purpose of demonstrating trends to divide them into illite-rich and smectite-rich clays.

There are three broad clay assemblages: (1) smectite-rich > illite-rich = kaolinite > chlorite; (2) illite-rich > smectite-rich > kaolinite > chlorite; (3) illite-rich > smectite-rich = kaolinite = chlorite. At very high proportions of illite and illite–smectite, kaolinite and chlorite are scarce or absent (category 3). The transition between the clay assemblages 1 and 2 is rapid, whereas between 2 and 3 it is gradational (Fig. 9). Clay assemblage 3 is typically green with some colour mottling, slickensided and calcareous (either nodular calcite or bioclasts) gley or pseudogley palaeosols. Clay assemblage 3 is typically grey, sometimes laminated, but never mottled or slickensided. Clay assemblages 2 and 3 occur in five distinct intervals of the Solent Group. These

intervals are around 10 m thick in clay-rich sediment and 15 m thick in the Bembridge Limestone, and all show high-frequency alternation of illite-rich and illite-poor clay assemblages (Fig. 9).

Interpretation

In the Hampshire Basin illitization cannot have occurred through burial diagenesis as maximum burial has not exceeded a few hundred metres (Gale *et al.* 1999). Huggett *et al.* (2001) suggested that the correlation between slickensides and mottling in gley palaeosols and high illitic clay content is the key to the origin of the illite. Slickensides are caused by movement of peds during wetting and drying (Retallack 2001). Colour mottling is also a consequence of drying out of the soil profile and reprecipitation of ferrous iron as ferric iron, a process that is not uniform, hence the mottled appearance. Experimental work by Srodon & Eberl (1984) and Eberl *et al.* (1986) has shown that wetting and drying of smectite, at surface temperature and pressure, fixes potassium irreversibly, with most layers collapsing in fewer than 40 cycles. Those workers found that smectite layers are converted to interstratified illite–smectite, and ultimately to illite. Huggett *et al.* (2001) suggested that the illite–smectite in the palaeosols of the Solent Group formed as a consequence of repeated wetting and drying of soils. Huggett & Cuadros (2005) have demonstrated that the probable driving mechanism was reduction of Fe³⁺ to Fe²⁺ during periods of waterlogging, resulting in irreversible layer charge increase and fixation of K⁺ in the interlayer sites. This probably occurred when seasonality contrast was at a maximum, with wet winters and dry summers.

Orbital tuning of clay mineralogical data

The previous section of this paper has demonstrated the stratigraphic variability inherent in the clay mineralogy of the Solent Group of Whitecliff Bay in the Isle of Wight, in particular the large variation of the illitic clay content (from 20% to 100%) that is thought to reflect variations in seasonal contrast (Fig. 9). The Whitecliff Bay Solent Group represents *c.* 2.5 Ma (Berggren *et al.* 1995), and therefore the large illitic clay peaks in Sequences 1–6 represent mean periods of 416 ka, which might correspond to climate forcing that arises from the Earth's variation in eccentricity with a period of 406 ka. This hypothesis is tested in the present study by attempting to match the variation in illitic clay with astronomical parameters. If the hypothesis of eccentricity forcing is correct, then the record should also reveal orbital variations at shorter time periods (*c.* 100 ka short eccentricity and 41 ka obliquity cycles). The astronomically tuned ages and relative durations can then be compared with independently obtained age constraints such as magneto- and biostratigraphic datum levels.

Tuning strategy and associated problems

Laskar (1990) demonstrated that the Solar System is chaotic and that current astronomical calculations are likely to be valid only for the last 10–20 Ma (Laskar 1999). This uncertainty affects the exact position of individual obliquity and precession cycles, which are also dependent on the slowdown of the Earth as a result of tidal effects (Palike & Shackleton 2000). It is therefore necessary to employ a different tuning strategy in the study of sediments of Palaeogene age as compared with those used in the Neogene and Quaternary. Laskar (1999) suggested that the *c.* 400 ka long eccentricity cycle is more stable over time than other orbital cycles, and that this cycle can therefore be used to

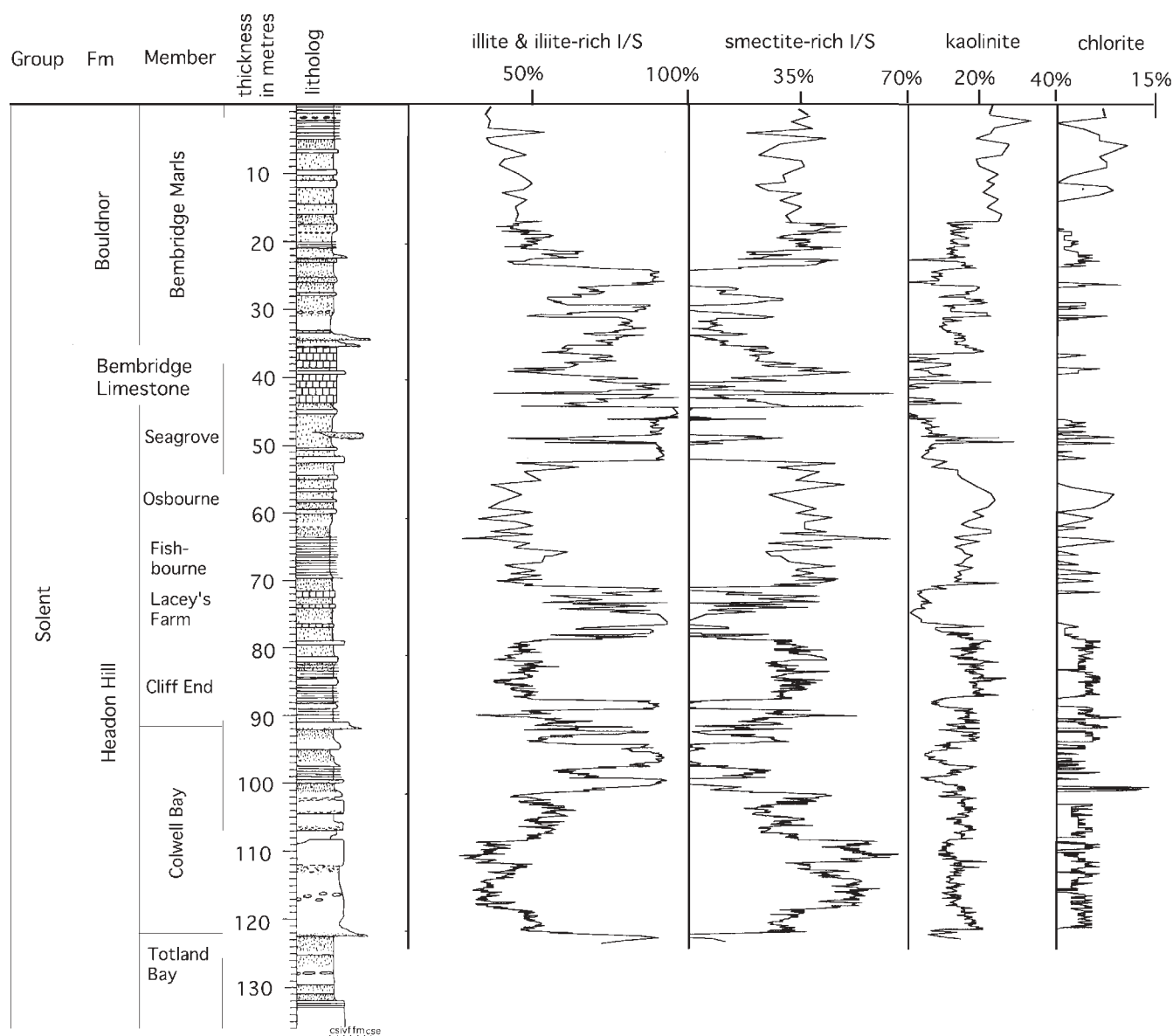


Fig. 9. Clay mineral percentages from the Solent Group in Whitecliff Bay, calculated by semi-quantitative XRD of the $<2 \mu\text{m}$ fraction. I/S, illite-smectite. (Note that the illite + illite-smectite column does not start at 0%.)

construct time scales far back into geological history. A new, improved astronomical solution has been calculated recently (Laskar 2001), which is used in this study to relate individual cycles in the clay mineralogy to *c.* 400 ka eccentricity cycles.

Because sedimentation rate is variable in the succession studied, it has been necessary to adjust some prominent illitic clay peaks on a *c.* 10 m to 2 m scale to short eccentricity (*c.* 100 ka period) and obliquity (*c.* 41 ka period) cycles, respectively. This is essentially a trade-off between demonstrating the presence of orbital cycles by adding additional tie-points, and being able to study the exact phase relationship between different cycles with as little as possible change to the original depth record. The time-series calibration and analysis was performed using the software AnalySeries (Paillard *et al.* 1996) and the SSA-Toolkit (Ghil *et al.* 2002).

Detailed tuning strategy and results

For the tuning, the total illitic clay content was used because this shows the clearest signal and never reaches values of zero. High values in authigenic illitic clay were interpreted to reflect an increased intra-annual seasonality (Singer 1984). The orbital configuration that maximizes seasonality has high eccentricity and obliquity values, with perihelion coinciding with summer. Therefore, high values in illitic clay were tuned to eccentricity maxima. To develop an age model, it was assumed that the base of the Bembridge normal polarity zone at -37 m in Whitecliff Bay succession corresponds to the start of Chron C13n. A possible hiatus within this polarity zone was noted, as its duration (*c.* 200 ka) is significantly shorter than that observed in marine sediments (*c.* 300–400 ka). This interpretation is supported by the presence of an incomplete illitic clay cycle at the base of

Sequence 6 in the lower Bembridge Marls (Fig. 6) and evidence of a sedimentological hiatus at the Bembridge Limestone–Bembridge Marl contact.

To fix the ‘floating’ time scale developed here in real time, the dataset was anchored to the 400 ka eccentricity cycle that is closest to published ages for the start of Chron C13n. This results in an age for the start of C13n (33.63 Ma) that is older than that given by Cande & Kent (1995; 33.545 Ma), but agrees fairly well with the revised age estimate given by Wei (1995; 33.812 Ma). The interval of reversed polarity between the base of the Bembridge normal polarity zone (start of C13n) and the top of the Headon Hill normal polarity zone at 87 m (end of C15n) contains 2.5 *c.* 400 ka eccentricity cycles, giving a duration of *c.* 1 Ma for C13r. This compares well with the 1.1 Ma duration assigned to C13r by Cande & Kent (1995) and Wei (1995).

Figure 10 shows that filters of the tuned dataset also recovered convincing short (100 ka) eccentricity cycles, but climatic precession cycles do not seem to be represented strongly in this succession. Sedimentation rates average *c.* 6–7 cm ka⁻¹ with a range generally within 5–10 cm ka⁻¹, and it was not necessary to infer the existence of large, rapid changes in the sedimentation rate to arrive at the tuning presented here.

Spectral analysis

Spectral analysis was performed on the ‘tuned’ dataset, employing the Multitaper Method of Thomson (1982), with five tapers and a taper \times bandwidth product of three (Fig. 11). The 95% confidence interval for the spectral estimate was computed using AnalySeries (Paillard *et al.* 1996), and the 90, 95 and 99% significance levels were computed from a red noise estimate, using the SSA-Toolkit software (Ghil *et al.* 2002). As expected, the spectrum (Fig. 11) shows a strong peak at around 400 ka, as well as convincing peaks for the shorter eccentricity cycle at around 100 ka, and a strong peak at the obliquity frequency (41 ka). This supports the hypothesis that the large-scale varia-

tions in clay mineralogy are linked to the orbital eccentricity cycles. Unfortunately, the length of the record and the quality of the data do not permit further statistical analysis such as complex demodulation. Table 2 shows the magneto- and biostratigraphic datum levels that were available in this study together with their assigned ages.

Discussion

Orbital controls on sedimentation, sea level and mineralogy

There is a precise correspondence between sequences in the Solent Group, as identified from sedimentological and faunal criteria (Figs. 4 and 5), and the 400 ka eccentricity cycle identified from spectral analysis of the illitic clay data (Figs. 10 and 11). In the Headon Hill and Bembridge Limestone Formations, periods of high eccentricity on the 400 ka cycle show evidence of overall low sea level, enhanced sea-level fluctuation and increased seasonal contrast (Figs. 4 and 9). The last is shown particularly well by the relative abundance of illitic clay, which formed in soils through repeated wetting and drying cycles (Huggett *et al.* 2001), and the abundance of the pulmonate gastropod *Galba*. In contrast, periods of low eccentricity correlate with brackish and marine transgressions. Sequence boundaries for Sequences 3–7 correspond to the maximum rate of rise of the 400 ka eccentricity cycle, and transgressive surfaces correspond to the maximum rate of decreased eccentricity (Fig. 10).

Short eccentricity and obliquity cycles were identified in the illitic clay time-series from the Whitecliff succession from the application of tuning and spectral analysis (Figs. 10 and 11). The illitic clay peaks that tune to obliquity correspond precisely to palaeosols at the summits of the 2–4 m thick fining upwards cycles interpreted here as tidal channel fills (e.g. Fig. 6). A plausible mechanism for the formation of these cycles is that obliquity controlled sea level through relatively minor fluctua-

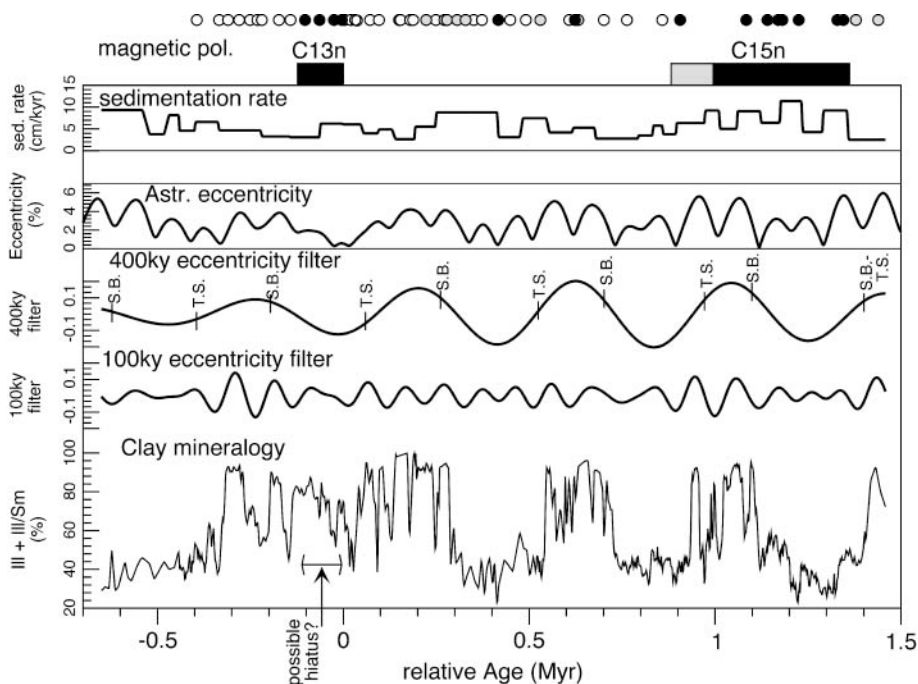


Fig. 10. The ‘tuned’ record of illitic clay (Ill + Ill/Sm, illite + illite–smectite) on a time scale, together with filters that extract the *c.* 400 ka and *c.* 100 ka components from this dataset. The eccentricity values from Laskar (2001, 2004) are shown for comparison. (Note how the individual 400 ka cycles that are present in the data were matched to the eccentricity curve.) The right column of this figure shows the sedimentation rates that result from our time scale. The position of magnetic reversals is indicated at the right-hand side of the figure. Considering that tuning was performed using eccentricity cycles, we estimate the associated error to be *c.* 100 ka. S.B., sequence boundary; T.S., transgressive surface.

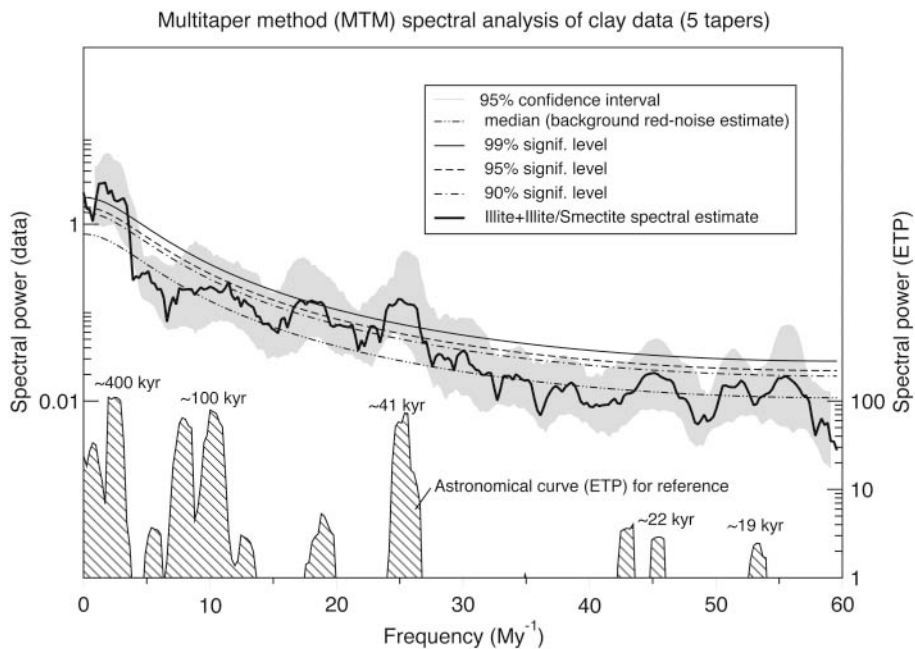


Fig. 11. Spectral estimates by the ‘Multitaper Method’ of Thomson (1982) of the ‘tuned’ dataset on a logarithmic power scale, with five tapers and a taper \times bandwidth product of three. We computed the 95% confidence interval for spectral estimate using AnalySeries (Paillard *et al.* 1996) and the 90, 95 and 99% significance levels from a red noise estimate, using the SSA-Toolkit (Ghil *et al.* 2002). Spectral peaks approximately match those predicted from astronomical observations (Laskar *et al.* 1993; Laskar 2001, 2004). The eccentricity (especially the 400 ka cycle) is most strongly expressed, with an additional highly significant peak at the obliquity (41 ka) component. Climatic precession is not strongly expressed. Various side lobes are attributed to spurious strong excursions in the signal. Additional significant power is present around *c.* 50 ka, which is another weaker component of the obliquity forcing. It is uncertain whether this peak really represents forcing or is an artificial side lobe. ETP, eccentricity, tilt and precession, normalized to the same variance

Table 2. Magneto- and biostratigraphical datum levels in the Whitecliff Bay Solent Group

Event	Depth (m)	Age herein (Ma)	Cande & Kent (1995)	Wei (1995)
Top C13n	31.4	33.503		
Base C13n	37.15	33.626	33.545	33.812
Top C15n	87	34.621	34.655	34.922
Base C15n	122.5	34.988		
NP19–20	122			

tions in the volume of Antarctic ice. Thus, the channels were initially cut by sea-level falls of one to several metres, and on the subsequent rise were progressively infilled and finally abandoned. Subsequently, pedogenic processes resulted in the formation of gley palaeosols and the neoformation of illitic clay by wetting and drying.

Global events in the Late Eocene–Early Oligocene

Studies of oxygen isotopes from numerous deep-sea cores demonstrates the existence in the Early Oligocene of a heavy $\delta^{18}\text{O}$ event of 1.5‰ (Oi-1; Miller *et al.* 1991; Zachos *et al.* 1996), which lasted *c.* 400 ka. The Oi-1 event commenced in the Late Eocene, *c.* 200 ka before the start of Chron 13n (Zachos *et al.* 1996; Fig. 8) and the maximum excursion coincides with the start of Chron 13n, thus shortly postdating (by about 100 ka) the Eocene–Oligocene boundary based on the extinction of the planktic foraminiferan *Hantkenina* (Berggren *et al.* 1995). The oxygen isotope event reflects both the rapid cooling of oceanic bottom waters and the concomitant growth of Antarctic ice (Zachos *et al.* 1996), and has been attributed primarily to a decline in atmospheric CO_2 values below a threshold level and secondarily to opening of the Drake Passage (Deconto & Pollard 2003). There is some doubt concerning the relative contributions of temperature and ice volume to the $\delta^{18}\text{O}$ excursion, but it is generally considered that Antarctic ice volume achieved at least

50% of its present development. It has been suggested that there should therefore be a large and rapid fall in sea level close to the Eocene–Oligocene boundary, estimated to be 30–90 m by Miller *et al.* (1991) and modelled more conservatively at 40–50 m in a recent study (Deconto & Pollard 2003).

This sea-level fall has been identified as the cause of a major early Oligocene unconformity dated to NP21–22 on the west African continental margin (Séranne 1999). Records of sea-level change across this interval in European successions were summarized by Vandenberghe *et al.* (2003). Those workers correlated sequence boundaries Pr3 and Ru1 as corresponding respectively to cooling events Oi-1a and Oi-1b (Zachos *et al.* 1996). They identified and correlated these events in marine sediments from Italy northwestwards through Europe to the North Sea Basin, but did not provide estimates of the amount of sea-level fall involved.

Coastal plain successions, such as that represented by the Solent Group, are very sensitive to sea-level change, and a rapid fall of 40–50 m or more should certainly register as a major incision event (e.g. Van Wagoner *et al.* 1988). Positive identification of the base of Chron 13n within the Bembridge Limestone Formation means that it should be possible to identify the position of major Eocene–Oligocene boundary events (recognized in deep-sea sediments) in the Whitecliff succession. This has been attempted by the identification of 41 ka obliquity cycles from the base of Chron 13n, and using these to establish a time scale (Fig. 12).

The sea-level fall that is identified high in the Seagrove Member beneath the Bembridge Limestone is interpreted as a response to the Early Oligocene eustatic event, about 150–160 ka before Chron 13n and thus probably coincident with the very commencement of Oi-1 (see Zachos *et al.* 1996). This conclusion is supported by independent evidence of a significant temperature fall at the same level in the Isle of Wight from various studies, including work on the size of charophyte oogonia (Sille *et al.* 2004). Oogonia of *Harrisichara* were found to increase in volume twofold, possibly in response to falling temperatures, between the upper Osborne Member and the lower Bembridge Limestone (Fig. 12), a larger change than at any other level in the Solent Group. Additionally, Grimes *et al.* (2005) recorded a 2‰ heavy shift in freshwater $\delta^{18}\text{O}$ values derived from rodent tooth enamel phosphate, the largest heavy event in the succession, between the Osborne Member and the Bembridge Limestone.

The sequence boundary at the base of Sequence 5, underlying the Bembridge Limestone, is marked by demonstrable incision in the proto-Solent drainage system of about 15 m. This is the largest fall found in the succession and the only one that was sufficiently large to transport abundant flints derived directly from the Chalk into the proto-Solent channel (Fig. 7). However, this value falls far short of even the most conservative estimates of sea-level fall associated with the Oi-1a event (30 m), a discrepancy possibly explained by suppression of incision by rapid subsidence rates (Davies & Gibling 2003).

It is noteworthy that this sequence boundary is related directly to the 400 ka eccentricity cycle, and is coincident with the maximum rate of rise in eccentricity values. The strength of the 400 ka cycle has been widely recognized in deep-sea Eocene–Oligocene sediments (Zachos *et al.* 1996). It is therefore suggested that the major build-up of ice on Antarctica during Oi-1 (e.g. Deconto & Pollard 2003) is related somehow to an orbital configuration of high eccentricity (see below).

The sea-level curve generated through the Late Eocene–Early Oligocene succession on the Isle of Wight shows how the 406 ka eccentricity cycle directly controls sequence formation. A progressive increase in the magnitude of sea-level change associated with successive 400 ka cycles is seen through the lower Solent

Group (Fig. 8), reaching a maximum value close to the base of the Oligocene in Sequence 5, and subsequently falling in Sequences 6 and 7. This pattern of sea-level change across the Eocene–Oligocene boundary offers comparisons with one of the model results of Deconto & Pollard (2003) in which the effects of subglacial processes are included in the history of ice build-up on Antarctica. The sub-glacial generation of new till on Antarctica caused progressively increasing, high-amplitude orbital variability through the Oi-1 isotope event (Deconto & Pollard 2003, fig. 2b, blue). This modelled scenario results in a gradual rise in orbitally moderated sea levels from 5 to 30+ m in the 1 Ma interval preceding Oi-1, followed by a progressive fall. The modelled pattern is comparable with the sea-level curve for the Whitecliff Bay succession (Fig. 8), but with about twice the values of sea-level change.

Milankovitch and sea level: general relationships

In the orbitally tuned Eocene–Oligocene succession described herein, there is a precise correspondence between the sequences, formed in response to sea-level change, and the 406 ka eccentricity cycle. This relationship has been noted also in Cretaceous strata (Strasser *et al.* 2000; Gale *et al.* 2002) and demonstrates that sea level was under direct climatic control in response to Milankovitch forcing in the Mesozoic and early Cenozoic. It is interesting that both the magnitude and rates of sea-level rises and falls associated with the 406 ka cycle (3–15 m) are very similar in the mid-Cretaceous (Cenomanian) and the Eocene–Oligocene, when Antarctic ice was certainly present. Therefore sea level may have been under glacioeustatic control even during the warm parts of the Cretaceous and Palaeogene (Gale *et al.* 2002; Miller *et al.* 2003).

Sea-level lowstands correspond to times of high orbital eccentricity in both the Solent Group and the Cenomanian (Gale *et al.* 2002), in contrast to the Quaternary, when ice-generated lowstands correlate precisely with low eccentricity (Pillans *et al.* 1998). This argument rests primarily upon our correct interpretation of sea-level change through sequence stratigraphical analysis. Models of the relationship between long eccentricity cycles and Mesozoic sea levels (Strasser *et al.* 2000) that are based on

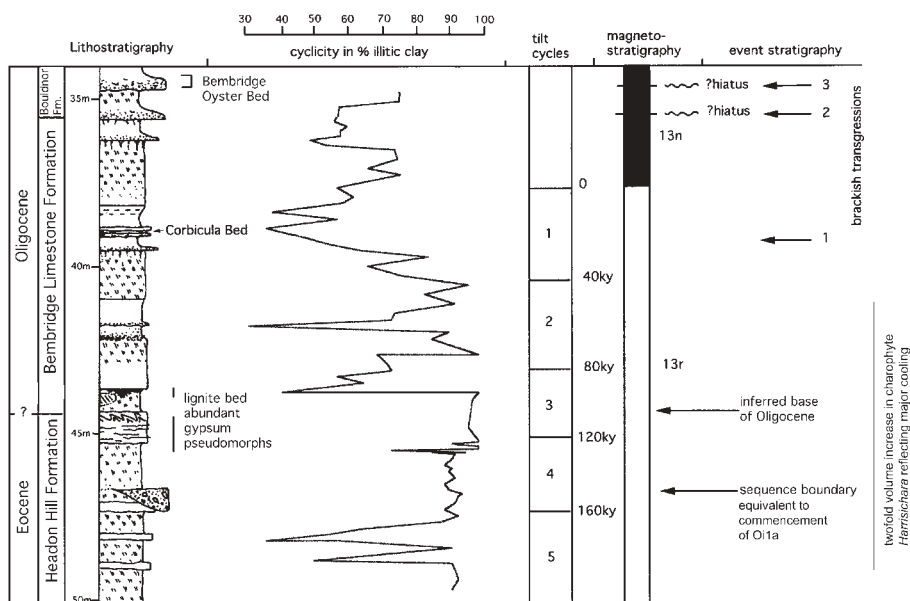


Fig. 12. Interpretation of Eocene–Oligocene boundary events, Whitecliff Bay. The percentage of illitic clay is used to identify obliquity cycles (41 ka), which are numbered downwards from the base of Chron 13n and provide a time scale for events. The major sea-level fall at the base of Sequence 5 occurred *c.* 150 ka before the start of Chron 13n, and probably reflects cooling associated with the Oi-1a event (Zachos *et al.* 1996). The base of the Oligocene is defined by the extinction of the planktonic foraminiferan *Hantkenina*, which reportedly disappeared 100 ka before the start of Chron 13n. The correlative level falls close to the base of the Bembridge Limestone.

the Quaternary model therefore appear to be incorrect. It is interesting that Deconto & Pollard (2002) have developed a model for the Cretaceous–Palaeogene in which the greatest variability in ice development occurs during periods of high eccentricity. South polar latitudes experience cool summers with minimal ablation when obliquity is low and precession places aphelion during austral summer. It seems possible that a complete reversal in the relationship between eccentricity and glaciation has taken place since the Palaeogene.

We would like to thank J. Backman for examining and commenting on nannofossil samples from the Isle of Wight. M. Gill (Mineralogy Department, Natural History Museum) kindly undertook the XRD analyses, and is gratefully acknowledged. We thank N. Shackleton for stimulating discussion.

References

- ARMENTEROS, L., DALEY, B. & GARCIA, E. 1997. Lacustrine and palustrine facies in the Bembridge limestone (late Eocene, Hampshire Basin) of the Isle of Wight, southern England. *Palaeogeography, Palaeoclimatology, Palaeoecology*, **128**, 111–132.
- AUBRY, M.-P. 1985. Northwestern European Palaeogene magnetostratigraphy, biostratigraphy, and paleogeography: calcareous nannofossil evidence. *Geology*, **13**, 198–202.
- BERGGREN, W.A., KENT, D.V., SWISHER, C.C. III & AUBRY, M.-P. 1995. A revised Paleogene geochronology and chronology. In: BERGGREN, W.A., KENT, D.V., AUBRY, M.-P. & HARDENBOL, J. (eds) *Geochronology, Time Scales and Stratigraphic Correlation: Framework for an Historical Geology*. Society of Economic Paleontologists and Mineralogists, Special Publications, **54**, 129–212.
- CANDE, S.C. & KENT, D.V. 1995. Revised calibration of the geomagnetic polarity timescale for the Late Cretaceous and Cenozoic. *Journal of Geophysical Research*, **100**, 6093–6095.
- COLLINSON, M.E. 1992. Vegetation and floristic changes around the Eocene–Oligocene boundary in western and central Europe. In: PROTHERO, D.R. & BERGGREN, W.A. (eds) *Eocene–Oligocene Climatic and Biotic Evolution*. Princeton University Press, Princeton, NJ, 437–450.
- DALEY, B. 1972. Macroinvertebrate assemblages from the Bembridge Marls (Oligocene) of the Isle of Wight, England, and their environmental significance. *Palaeogeography, Palaeoclimatology, Palaeoecology*, **11**, 11–32.
- DALEY, B. 1999. Palaeogene sections on the Isle of Wight. A revision of their description and significance in the light of research undertaken over recent decades. *Tertiary Research*, **19**, 1–69.
- DALEY, B. & EDWARDS, N. 1990. The Bembridge Limestone (Late Eocene), Isle of Wight, southern England. *Tertiary Research*, **12**, 51–64.
- DAVIES, J. & GIBLING, M.R. 2003. Architecture of coastal and alluvial deposits in an extensional basin; the Carboniferous Joggins Formation of eastern Canada. *Sedimentology*, **50**, 415–439.
- DECONTO, R.M. & POLLARD, D. 2002. Cretaceous ice sheets: a modelling perspective. In: BICE, K.L. (ed.) *Workshop on Cretaceous Climate and Ocean Dynamics, Florissant, Colorado, July 2002. Program, Abstracts, Field Guide*. 17.
- DECONTO, R.M. & POLLARD, D. 2003. Rapid Cenozoic glaciation of Antarctica induced by declining atmospheric CO₂. *Nature*, **421**, 245–249.
- EBERL, D.D., SRODON, J. & NORTHROP, H.R. 1986. Potassium fixation in smectite by wetting and drying. In: DAVIS, A. & HAYES, K.F. (eds) *Geochemical Processes at Mineral Surfaces*. American Chemical Society Symposium Series, **323**, 296–326.
- ELLIS, A.E. 1969. *British Snails*. Clarendon Press, Oxford.
- FORBES, E. 1853. On the fluvio-marine Tertiaries of the Isle of Wight. *Quarterly Journal of the Geological Society of London*, **9**, 259–270.
- GALE, A.S., JEFFREY, P.A., HUGGETT, J.M. & CONOLLY, P. 1999. Eocene inversion history of the Sandown Pericline, Isle of Wight, southern England. *Journal of the Geological Society, London*, **156**, 327–339.
- GALE, A.S., HARDENBOL, J., HATHWAY, B., KENNEDY, W.J., YOUNG, J.R. & PHANSALKAR, V. 2002. Global control of Cenomanian (Upper Cretaceous) sequences: evidence for Milankovitch control on sea level. *Geology*, **30**, 291–294.
- GHIL, M., DETTINGER, K. & IDE, K. ET AL. 2002. Advanced spectral methods for climatic time series. *Review of Geophysics*, **40**, Article 1003.
- GILKES, R.J. 1968. Clay mineral provinces in the Tertiary sediments of the Hampshire basin. *Clay Minerals*, **7**, 351–361.
- GRIMES, S.T., HOOKER, J.J., COLLINSON, M.E. & MATTEY, D.P. 2005. Summer temperatures of late Eocene to early Oligocene freshwaters. *Geology*, **33**, 189–192.
- HAILWOOD, E.A. 1989. *Magnetostratigraphy*. Geological Society of London, Special Report, **19**.
- HOOKE, J.J. 1992. British mammalian paleocommunities across the Eocene–Oligocene transition and their environmental implications. In: PROTHERO, D.R. & BERGGREN, W.A. (eds) *Eocene–Oligocene Climatic and Biotic Evolution*. Princeton University Press, Princeton, NJ, 494–515.
- HOOKE, J.J., COLLINSON, M.E., VAN BERGEN, P.F., SINGER, R.L., DE LEEUW, J.W. & JONES, T.P. 1995. Reconstruction of land and freshwater palaeoenvironments near the Eocene–Oligocene boundary, southern England. *Journal of the Geological Society, London*, **152**, 449–468.
- HOOKE, J.J., COLLINSON, M.E. & SILLE, N.P. 2004. Eocene–Oligocene mammalian faunal turnover in the Hampshire Basin, UK: calibration to the global timescale and the major cooling event. *Journal of the Geological Society, London*, **161**, 161–172.
- HUGGETT, J.M. & CUADROS, J. 2005. Low-temperature illitisation of smectite in the Late Eocene and Early Oligocene of the Isle of Wight (Hampshire Basin), U.K. *American Mineralogist*, **90**, 1192–1202.
- HUGGETT, J.M., GALE, A.S. & CLAUER, N. 2001. The nature and origin of non-marine 10-Å green clays from the late Eocene and Oligocene of the Isle of Wight (Hampshire basin). *UK Clay Minerals*, **36**, 447–464.
- INSOLE, A. & DALEY, B. 1985. A revision of the lithostratigraphical nomenclature of the Late Eocene and Early Oligocene strata of the Hampshire Basin, southern England. *Tertiary Research*, **7**, 67–100.
- KEENE, M.C. 1977. Ostracod assemblages and the depositional environments of the Headon, Osborne and Bembridge Beds (upper Eocene) of the Isle of Wight. *Palaeontology*, **20**, 405–445.
- KIRSHVINK, J.L. 1980. The least squares line and plane and analysis of palaeomagnetic data. *Geophysical Journal of the Royal Astronomical Society*, **62**, 699–718.
- LASKAR, J. 1990. The chaotic motion of the solar system—a numerical estimate of the size of chaotic zones. *Icarus*, **88**, 266–291.
- LASKAR, J. 1999. The limits of Earth orbital calculations for geological time-scale use. *Philosophical Transactions of the Royal Society of London, Series A*, **357**, 1733–1734.
- LASKAR, J. 2001. Astronomical solutions for paleoclimatic studies. *EOS Transactions, American Geophysical Union, Fall Meeting Supplement*, **82**, Abstract U11A-01.
- LASKAR, J., JOUTEL, F. & BOUDIN, F. 1993. Orbital, precessional and insolation quantities for the Earth from –20 Myr to +10 Myr. *Astronomical Astrophysics*, **270**, 522–533.
- LIENGJAREN, M., COSTA, L. & DOWNIE, C. 1980. Dinoflagellate cysts from the Upper Eocene–Lower Oligocene of the Isle of Wight. *Palaeontology*, **23**, 475–499.
- LOWRIE, W. 1990. Identification of ferromagnetic minerals in a rock by coercivity and unblocking temperature properties. *Geophysical Research Letters*, **17**, 159–162.
- MARTINI, E. 1970. The Upper Eocene Brockenhurst Bed. *Geological Magazine*, **107**, 225–228.
- MCELHINNY, M.W. 1964. Statistical significance of the fold test in palaeomagnetism. *Geophysical Journal of the Royal Astronomical Society*, **8**, 338–340.
- MILLER, K.G., WRIGHT, J.D. & FAIRBANKS, R.G. 1991. Unlocking the ice-house: Oligocene–Miocene oxygen isotopes, eustasy, and margin erosion. *Journal of Geophysical Research*, **96**, 6829–6848.
- MILLER, K.G., SUGARMAN, P.J. & BROWNING, J.V. ET AL. 2003. Late Cretaceous chronology of large, rapid sea-level changes: glacioeustasy during the greenhouse world. *Geology*, **31**, 585–588.
- PAILLARD, D., LAYBERIE, L. & YU, P. 1996. Macintosh program performs time-series analysis. *EOS Transactions, American Geophysical Union*, **77**, 379.
- PALIKÉ, H. & SHACKLETON, N.J. 2000. Constraints on astronomical parameters from the geological record for the last 25 Ma. *Earth and Planetary Science Letters*, **182**, 1–14.
- PAUL, C.R.C. 1989. The molluscan faunal succession in the Hatherwood Limestone Member (Upper Eocene), Isle of Wight. *Tertiary Research*, **10**, 147–162.
- PILLANS, B., CHAPPELL, J. & NAISH, T.R. 1998. A review of Milankovitch climatic beat; template for Plio-Pleistocene sea-level changes and sequence stratigraphy. *Sedimentary Geology*, **122**, 5–21.
- POMEROL, C. 1982. *The Cenozoic Era. Tertiary and Quaternary*. Chichester: Wiley; New York: Ellis Harwood.
- RETALLACK, G.R. 2001. *Soils of the Past*. Blackwell Science, Oxford.
- SCHUMM, S.A. 1993. River response to baselevel change: implications for sequence stratigraphy. *Journal of Geology*, **101**, 279–294.
- SÉRANNE, M. 1999. Early Oligocene stratigraphic turnover on the west Africa continental margin: a signature of the Tertiary greenhouse-to-icehouse transition? *Terra Nova*, **11**, 135–140.
- SHACKLETON, N.J., HAGELBERG, T.K. & CROWHURST, S.J. 1995. Evaluating the success of astronomical tuning: pitfalls of using coherence as a criterion for

- assessing pre-Pleistocene timescales. *Paleoceanography*, **10**, 693–697.
- SHACKLETON, N.J., CROWHURST, S., WEEDON, G.P. & LASKAR, J. 1999. Astronomical calibration of Oligocene–Miocene time. *Philosophical Transactions of the Royal Society of London, Series A*, **357**, 1907–1929.
- SILLE, N.P., COLLINSON, M.E., KUCERA, M. & HOOKER, J.J. 2004. Evolution within the charophyte genus *Harrisichara*, Late Palaeogene, southern England: environmental and biostratigraphic implications. *Palaeogeography, Palaeoclimatology, Palaeoecology*, **208**, 153–173.
- SINGER, A. 1984. The paleoclimatic interpretation of clay minerals in sediments—a review. *Earth-Science Reviews*, **21**, 251–293.
- SRODON, J. & EBERL, D.D. 1984. Illite. In: BAILEY, S.W. (ed.) *Micas*. Mineralogical Society of America, Reviews in Mineralogy, **13**, 495–544.
- STEENBRINK, J., VAN VUGT, N., HILGEN, F.J., WJBRANS, J.R. & MEULENKAMP, J.E. 1999. Sedimentary cycles and volcanic ash beds in the lower Pliocene lacustrine successions of Ptolemais (NW Greece): discrepancy between $^{40}\text{Ar}/^{39}\text{Ar}$ and astronomical ages. *Palaeogeography, Palaeoclimatology, Palaeoecology*, **152**, 283–303.
- STRASSER, A., HILLGARTNER, H., HUG, H. & PITTER, B. 2000. Third order depositional sequences reflecting Milankovitch cyclicity. *Terra Nova*, **12**, 303–311.
- THOMSON, D.J. 1982. Spectrum estimation and harmonic analysis. *Proceedings of the IEEE*, **70**, 1055–1096.
- TOWNSEND, H.A. & HAILWOOD, E.A. 1985. Magnetostratigraphic correlation of Palaeogene sediments in the Hampshire and London Basins, southern UK. *Journal of the Geological Society, London*, **142**, 957–982.
- VANDENBERGHE, N., BRINKHUIS, H. & STEURBAUT, E. 2003. The Eocene/Oligocene boundary in the North Sea Area: a sequence stratigraphic approach. In: PROTHERO, D.R., IVANY, L.C. & NESBITT, E.A. (eds) *From Greenhouse to Icehouse. The Marine Eocene–Oligocene Transition*. Columbia University Press, New York, 419–438.
- VAN VUGT, N., STEENBRINK, J., LANGEREIS, C.G., HILGEN, F.J. & MEULENKAMP, J.E. 1998. Magnetostratigraphy based astronomical tuning of the Early Pliocene lacustrine sediments of Ptolemais (NW Greece) and bed to bed correlation to the marine record. *Earth and Planetary Science Letters*, **164**, 535–551.
- VAN WAGONER, J.C., POSAMENTIER, H.W., MITCHUM, R.M., VAIL, P.R., SARG, J.F., LOUTIT, J.S. & HARDENBOL, J. 1988. An overview of the fundamentals of sequence stratigraphy and key definitions. In: WILGUS, C.K., HASTINGS, B.S., POSAMENTIER, H.W., ROSS, C.A., VAN WAGONER, J.C. & KENDALL, C.G.St.C. (eds) *Sea Level Changes: an Integrated Approach*. Society of Economic Paleontologists and Mineralogists, Special Publications, **42**, 39–45.
- WEI, W. 1995. Revised age calibration points for the geomagnetic polarity time scale. *Geophysical Research Letters*, **22**, 957–960.
- WHITE, H.J.O. 1921. *A Short Account of the Geology of the Isle of Wight*. Memoirs of the Geological Survey of Great Britain.
- ZACHOS, J.C., QUINN, T.M. & SALAMY, K.A. 1996. High-resolution (104 years) deep-sea foraminiferal stable isotope records of the Eocene–Oligocene climate transition. *Paleoceanography*, **11**, 251–266.

Received 14 November 2003; revised typescript accepted 29 July 2005.
Scientific editing by John Howell